



Contents lists available at ScienceDirect

International Journal of Rock Mechanics & Mining Sciences

journal homepage: www.elsevier.com/locate/ijrmms

Technical Note

An analytical solution for recovering the complete *in-situ* stress tensor from Flat Jack tests



Ben-Guo He, Yossef H. Hatzor*

Department of Geological and Environmental Sciences, Ben-Gurion University of the Negev, Beer-Sheva 84105, Israel

ARTICLE INFO

Article history:

Received 5 January 2015

Received in revised form

15 April 2015

Accepted 19 May 2015

1. Introduction

In-situ stress determination has a dominant role in the design of underground construction projects as the initial and excavation induced stress concentrations typically affect the performance of the rock mass surrounding the excavation. While it is possible to estimate the initial and excavation induced stresses from theory using some well accepted assumptions, accurate determination of the stress tensor near the excavation face typically requires either direct measurements or back analyses.

One of the earliest methods used in rock mechanics for *in-situ* stress measurement is the Flat Jack method, the principles of which are described in the collection of ISRM suggested methods^[1] and reviewed among other techniques by Fairhurst.^[2] The method was first proposed by Mayer^[3] and later improved by Rocha^[4] and Hoskins^[5]. Based on the stress relief principle, the cancellation pressure is used to obtain the *in-situ* stress component acting normal to the Flat Jack plate^[6,7].

The Flat Jack method is a “cancellation” *in-situ* stress test method, in which a thin slot is cut into the rock surrounding an underground opening and a pressure gage is inserted into the slot (Fig. 1a). The pressure in the flat jack is increased until the recorded strain relaxation of the sidewall is cancelled (Fig. 1b). The jack pressure at which the strain relaxation is cancelled, is assumed to be the normal stress acting on the face of the flat jack. Therefore, with known solutions for stress concentrations around the opening, the initial *in-situ* stress field can be recovered by means of inversion, if a sufficient number of flat jack tests are performed around the opening, at different orientations. The following assumptions are made in the solution process: the width of the slot is very small with respect to the span of the opening, the

elastic modulus of the rock is linear and reversible in the range of stresses of interest, the rock mass is isotropic, there is perfect coupling between the flat jack and the rock which is typically achieved using cement filling between the jack and the rock.

The method has been used in many case studies around the world. A set-up of a total of twelve slots cut along the wall of an underground opening was recommended by Pinto and Cunha^[8] to obtain the stress tensor. Franco et al.^[9] used the method to back analyze the 3D stress tensor via the least square method in the Serra Sa Mesa Hydroelectric Power Plant in Brazil. Results of twelve Flat Jack tests performed in an underground hydroelectric power project in northern Portugal have been integrated into a stress model that took into account both topography and tectonic effects^[10]. Similarly, the *in-situ* stress field of the Gardanne basin in France was assessed using the Flat Jack method where eleven stress measurements were carried out at different depths^[11]. In Italy, 60 tests were carried out during six geomechanical investigation campaigns performed for construction of five large underground power plants by the Italian Electricity Board^[12].

Most of the current procedures for determination of the *in-situ* stress tensor from the Flat Jack method are based on a two-dimensional analytical solution, in which the orientation of one principal stress is usually assumed to be parallel to the axis of the investigated gallery. If the far field principal stresses are assumed to be horizontal and vertical, then only two flat jack tests are necessary to obtain the magnitude of the principal stresses by direct application of Kirsch solution [13], as shown by Goodman^[7]; see Fig. 2. Amadei and Stephansson^[6] proposed a three-dimensional solution for a transversely isotropic medium where they assume that the stress at every point has one elastic axis of symmetry which is aligned with the tunnel axis direction (Fig. 3). The solution is provided in complex variable functions. Ultimately, the solution for the isotropic case is provided by Amadei and Stephansson^[6] for three out of the six components of the far field

* Corresponding author.

E-mail address: hatzor@bgu.ac.il (Y.H. Hatzor).

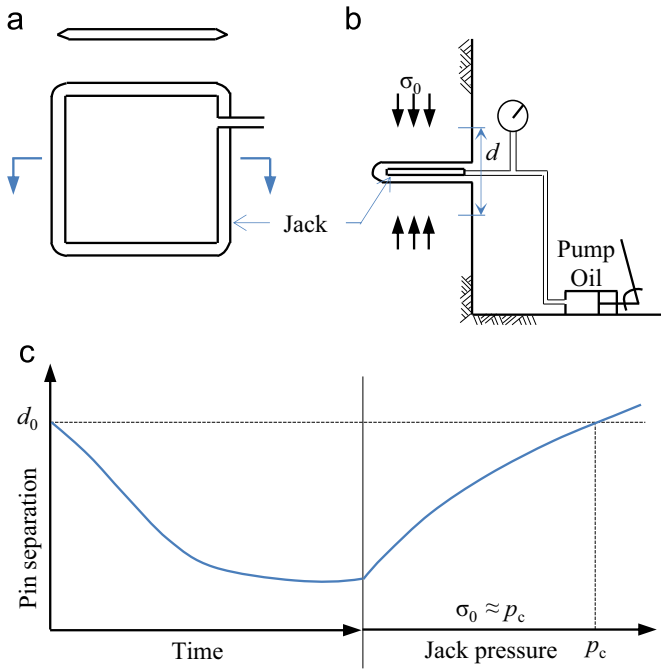


Fig. 1. Principles of the Flat Jack test: (a) Plan view and cross section of flat jack. (b) Cross section through the side wall of a tunnel showing the flat jack test assembly. (c) Pin separation curve (modified after Ref. [7]).

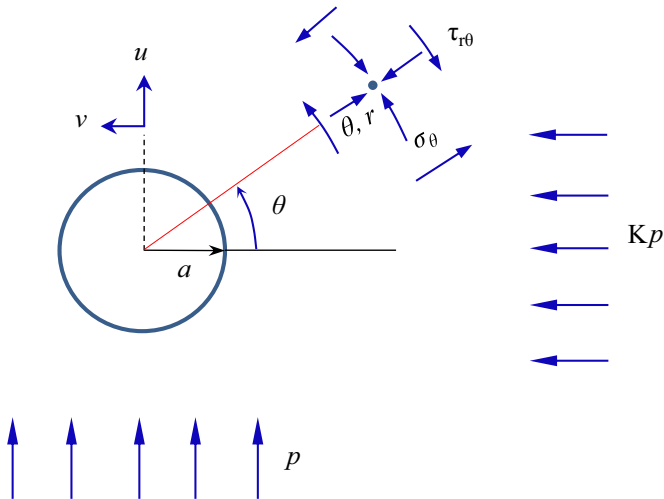


Fig. 2. Stresses around a circular hole in polar coordinates under horizontal and vertical far field Principles stresses (modified after Ref. [7]).

stress tensor, where θ_i ($i=1, 2, 3$) is the angle defining the position of the Flat Jack test from the x -axis (Fig. 4):

$$\begin{pmatrix} \sigma_{\theta 1} \\ \sigma_{\theta 2} \\ \sigma_{\theta 3} \end{pmatrix} = \begin{pmatrix} 1 - \cos 2\theta_1 & 1 + \cos 2\theta_1 & -4 \sin 2\theta_1 \\ 1 - \cos 2\theta_2 & 1 + \cos 2\theta_2 & -4 \sin 2\theta_2 \\ 1 - \cos 2\theta_3 & 1 + \cos 2\theta_3 & -4 \sin 2\theta_3 \end{pmatrix} \cdot \begin{pmatrix} \sigma_x \\ \sigma_y \\ \tau_{xy} \end{pmatrix} \quad (1)$$

A complete three-dimensional solution, the derivation of which is not provided, for the far field stress tensor was suggested by Pinto and Cunha^[8] where at every point θ around the tunnel axis four tests must be performed at four inclination angles α with respect to the direction vector r , separated at 45° intervals (Fig. 5).

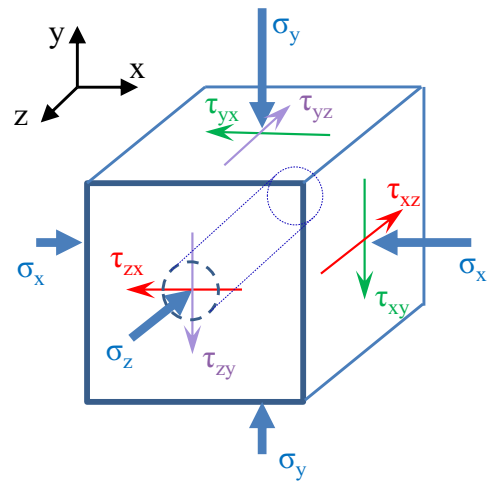


Fig. 3. Three-dimensional far field stress tensor and a circular tunnel aligned with the z axis.

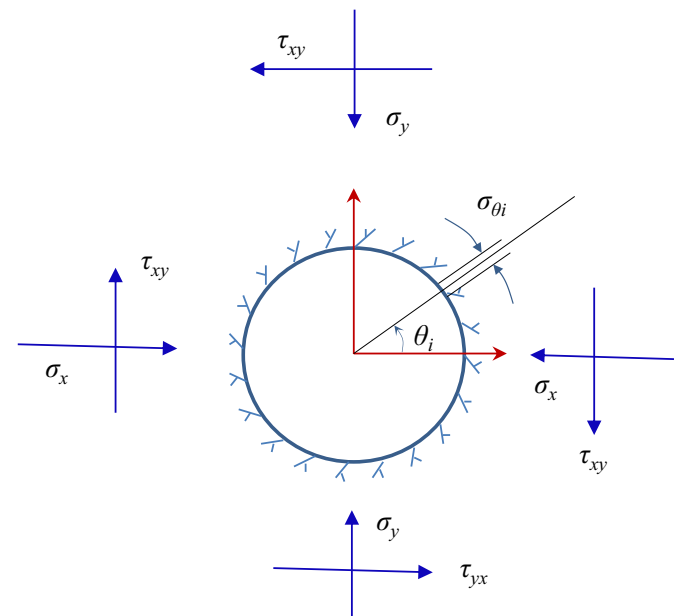


Fig. 4. Sign convention used in Ref. [6] for Flat Jack test i ($i=1, 2, 3$) performed around a circular opening subjected to far field stress tensor.

In this approach, 12 tests are needed to resolve the complete far field stress tensor, to be performed at three different θ positions around the tunnel axis. This procedure requires at every θ position four slots one close to another and this may adversely affect the accuracy of the solution due to possible interactions between the slots.

In this note we present an analytical solution for recovering the six components of the far field stress tensor in an isotropic rock mass using only six Flat Jack tests to be performed at a minimum of three different θ positions around the tunnel axis and a minimum of three α inclinations around the tunnel radius vector. No assumptions need to be made with respect to the orientation of the initial far field stresses. The complete derivation of the analytical solution we propose is provided below.

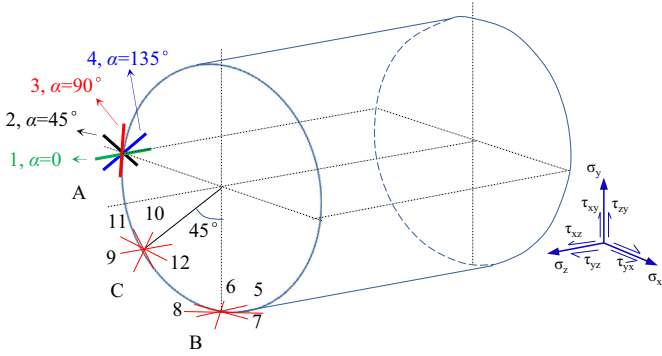


Fig. 5. Procedure proposed in Ref. [8] for determination of the far field stress tensor in which 12 tests are required.

2. Stress distribution around a circular hole in the x-y plane

It can be shown (for complete derivation see Appendix A) that the stress distribution around a circular hole in cylindrical coordinates may be expressed as

$$\left. \begin{aligned} \sigma_r &= \frac{\sigma_x + \sigma_y}{2} \left(1 - \frac{a^2}{r^2}\right) + \frac{\sigma_x - \sigma_y}{2} \left(1 - \frac{a^2}{r^2}\right) \left(1 - \frac{3a^2}{r^2}\right) \cos 2\theta + \tau_{xy} \left(1 - \frac{a^2}{r^2}\right) \left(1 - \frac{3a^2}{r^2}\right) \sin 2\theta \\ \sigma_\theta &= \frac{\sigma_x + \sigma_y}{2} \left(1 + \frac{a^2}{r^2}\right) - \frac{\sigma_x - \sigma_y}{2} \left(1 + \frac{3a^4}{r^4}\right) \cos 2\theta - \tau_{xy} \left(1 + \frac{3a^4}{r^4}\right) \sin 2\theta \\ \tau_{r\theta} &= \tau_{\theta r} \\ &= -\frac{\sigma_x - \sigma_y}{2} \left(1 - \frac{a^2}{r^2}\right) \left(1 + \frac{3a^2}{r^2}\right) \sin 2\theta + \tau_{xy} \left(1 - \frac{a^2}{r^2}\right) \left(1 + \frac{3a^2}{r^2}\right) \cos 2\theta \end{aligned} \right\} \quad (2)$$

where θ is measured as in Fig. 4, a is the radius of circular opening. Letting r equal a we obtain the same solution for σ_θ as proposed by Amadei and Stephansson^[6] for the immediate wall of the tunnel:

$$\begin{aligned} \sigma_\theta &= \sigma_x + \sigma_y - 2(\sigma_x - \sigma_y) \cos 2\theta - 4\tau_{xy} \sin 2\theta \\ &= [1 - 2 \cos 2\theta \quad 1 + 2 \cos 2\theta \quad -4 \sin 2\theta] \\ &\quad \begin{bmatrix} \sigma_x \\ \sigma_y \\ \tau_{xy} \end{bmatrix} \end{aligned} \quad (3)$$

The complete analytical solution which is derived in the appendix and shown in Eq. (2) is identical to Eq. (1) suggested by Amadei and Stephansson^[6], provided that the slots of the jack are parallel to tunnel axis, thus yielding σ_x , σ_y and τ_{xy} in the x-y plane (the tunnel cross section; see Fig. 4) based on three different tests. To obtain the remaining three components of the stress tensor, at least three more tests are necessary. In this note we propose a procedure in which the jack slots in the additional three tests are not necessarily parallel to the tunnel axis but rather form an angle α with respect to tunnel axis, as originally proposed by Pinto and Cunha^[8]. The angle α can be viewed as a rotation angle around the tunnel radius vector. Note that the angle α around the tunnel radius vector is measured clockwise from the tunnel axis to the slot when the system is viewed from outside the tunnel (Fig. 6). When

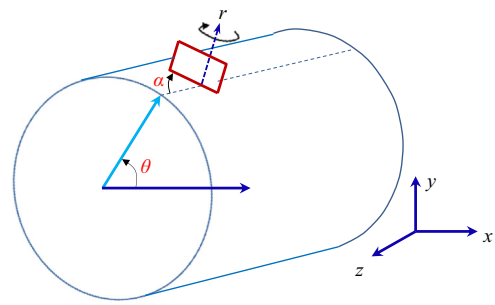


Fig. 6. Definition of the rotation angle α around tunnel radius vector r . Note that α is measured clockwise from tunnel axis (dashed line) when viewing the tunnel from the outside. From viewed from the inside of the tunnel (the field case) α is measured counterclockwise with respect to tunnel axis.

viewed from the inside of the tunnel, as would be the case in practice, α is measured counterclockwise with respect to the tunnel axis. Also note that here the slots are always perpendicular to the tunnel wall, as in previous procedures.

In our proposed procedure a total of only six tests is required, in contrast to a minimum of 12 tests that are required in the procedure proposed by Pinto and Cunha^[8]. We believe this represents a significant improvement, as possible interferences between the four slots in each measurement point in Pinto and Cunha procedure are avoided.

3. Finding the stress tensor components in the in z-direction

To obtain the stress components in the z-direction (σ_z , τ_{zx} and τ_{zy}) we rotate the coordinate system around the r axis (Fig. 7) to establish the relationship between σ_θ and the far field stress in the z-direction, thus the six components of the *in-situ* stress tensor can be determined.

3.1. Transformation of field variables from Cartesian to Cylindrical coordinates

We begin by rotating the x-y coordinate system around the z axis (Fig. 8). The rotation matrix for this case is

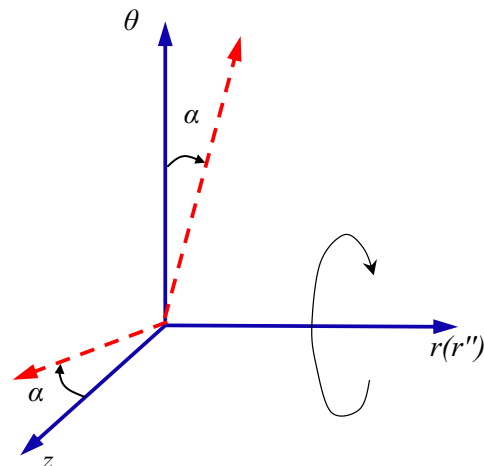


Fig. 7. Coordinate transformation rotation around r axis.

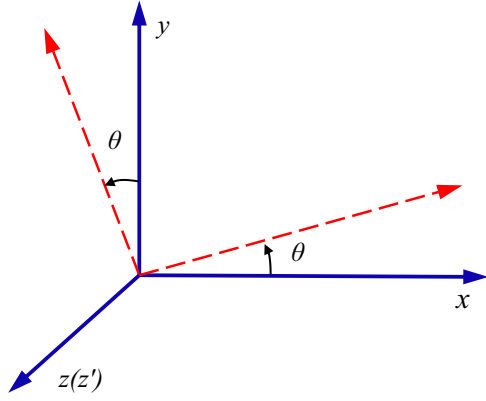


Fig. 8. Second order tensor coordination transformation.

$$Q_{ij} = \begin{bmatrix} \cos \theta & \sin \theta & 0 \\ -\sin \theta & \cos \theta & 0 \\ 0 & 0 & 1 \end{bmatrix} \quad (4)$$

Employing the second-order matrix transformation of isotropic tensor between Cartesian coordinate systems [e.g. Ref. [14]], we obtain:

$$\begin{aligned} \sigma(r, \theta, z) &= Q_{ij} \times \sigma(x, y, z) \times Q_{ij}^T \\ &\times \begin{bmatrix} \sigma_r & \tau_{r\theta} & \tau_{rz} \\ \text{symm} & \sigma_\theta & \tau_{\theta z} \\ & & \sigma_z \end{bmatrix} = \begin{bmatrix} \cos \theta & \sin \theta & 0 \\ -\sin \theta & \cos \theta & 0 \\ 0 & 0 & 1 \end{bmatrix} \\ &\times \begin{bmatrix} \sigma_x & \tau_{xy} & \tau_{xz} \\ \text{symm} & \sigma_y & \tau_{yz} \\ & & \sigma_z \end{bmatrix} \times \begin{bmatrix} \cos \theta & \sin \theta & 0 \\ -\sin \theta & \cos \theta & 0 \\ 0 & 0 & 1 \end{bmatrix}^T \\ &= \begin{bmatrix} \cos \theta \sigma_x + \sin \theta \tau_{yx} & \cos \theta \tau_{xy} + \sin \theta \sigma_y & \cos \theta \tau_{xz} + \sin \theta \tau_{yz} \\ -\sin \theta \sigma_x + \cos \theta \tau_{yx} & -\sin \theta \tau_{xy} + \cos \theta \sigma_y & -\sin \theta \tau_{xz} + \cos \theta \tau_{yz} \\ \tau_{zx} & \tau_{zy} & \sigma_z \end{bmatrix} \\ &\times \begin{bmatrix} \cos \theta & -\sin \theta & 0 \\ \sin \theta & \cos \theta & 0 \\ 0 & 0 & 1 \end{bmatrix} \end{aligned} \quad (5)$$

Using Eq. (5), we can now express $\tau_{\theta z}$ as

$$\tau_{\theta z} = -\sin \theta \tau_{zx} + \cos \theta \tau_{zy} \quad (6)$$

3.2. Local change in σ_z due to tunneling

Assuming there is no excavation induced deformation along the tunnel axis in the z-direction, we may write $\Delta \epsilon_z = [\Delta \sigma_z - \nu \Delta (\sigma_x + \sigma_y)] / E = 0$, where ν is Poisson's ratio. We can now find the excavation induced change in σ_z near the tunnel:

$$\Delta \sigma_z = \nu \Delta (\sigma_x + \sigma_y) = \nu [(\sigma_x + \sigma_y) - (\sigma_x' + \sigma_y')] \quad (7)$$

where σ_x' and σ_y' are the local stresses near the tunnel after excavation. Employing the first stress invariant, we may write:

$$\sigma_y' + \sigma_x' = \sigma_r + \sigma_\theta \quad (8)$$

Substituting Eq. (8) into Eq. (7), we can find the change in σ_z due to tunneling:

$$\begin{aligned} \Delta \sigma_z &= \nu \Delta (\sigma_x + \sigma_y) \\ &= \nu [(\sigma_x' + \sigma_y') - (\sigma_x + \sigma_y)] \\ &= \nu [(\sigma_r + \sigma_\theta) - (\sigma_x + \sigma_y)] \\ &= -\nu \left[2(\sigma_x - \sigma_y) \frac{a^2}{r^2} \cos 2\theta + 4\tau_{xy} \frac{a^2}{r^2} \sin 2\theta \right] \end{aligned} \quad (9)$$

Thus, the normal stress in the z direction near the tunnel after the excavation can be presented by the original stress components $\sigma_x, \sigma_y, \sigma_z$ and τ_{xy} as follows:

$$\begin{aligned} \sigma_z' &= \sigma_z + \Delta \sigma_z = \sigma_z - \nu \left[2(\sigma_x - \sigma_y) \frac{a^2}{r^2} \cos 2\theta + 4\tau_{xy} \frac{a^2}{r^2} \sin 2\theta \right] \\ &= -2\nu \frac{a^2}{r^2} \cos 2\theta \sigma_x + 2\nu \frac{a^2}{r^2} \cos 2\theta \sigma_y - 4\nu \frac{a^2}{r^2} \sin 2\theta \tau_{xy} + \sigma_z \end{aligned} \quad (10)$$

Note that the value of Poisson's ratio is needed for characterizing the change in stress in the z-direction induced by tunneling.

3.3. Rotation of the cylindrical coordinate system about the r axis

From Eqs. (2) and (10), the stress components at the wall of a circular tunnel of radius a ($r=a$) are

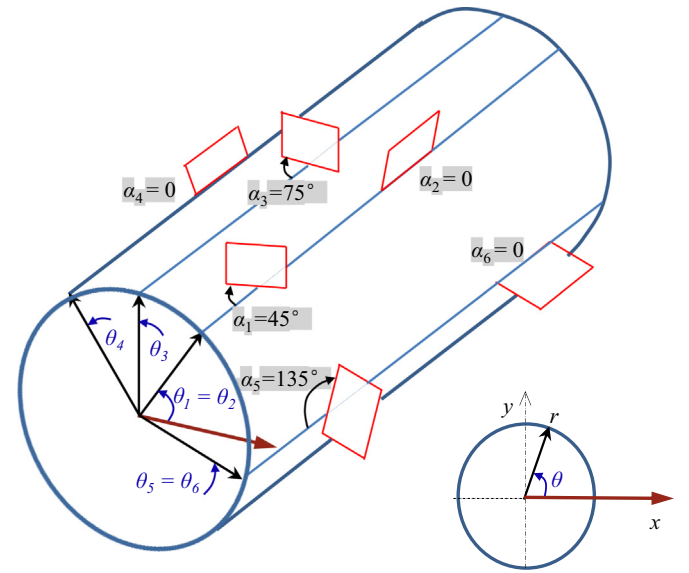
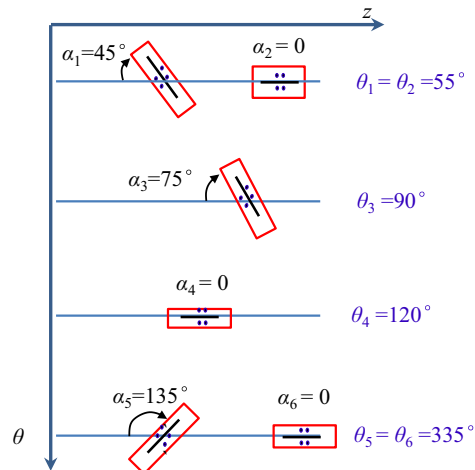


Fig. 9. Definition of angles to locate the slots of the Flat Jack tests: α inclination around the tunnel radius vector r ; θ dip around the tunnel.



$$\left. \begin{aligned} \sigma_r &= 0 \\ \sigma_\theta &= \sigma_x + \sigma_y - 2(\sigma_x - \sigma_y)\cos 2\theta - 4\tau_{xy} \sin 2\theta \\ \tau_{r\theta} &= \tau_{\theta r} = 0 \\ \sigma_z' &= \sigma_z - \nu[2(\sigma_x - \sigma_y)\cos 2\theta + 4\tau_{xy} \sin 2\theta] \end{aligned} \right\} \quad (11)$$

The stress matrix in the tunnel cross section where $r=a$ is

$$\sigma(r, \theta, z) = \begin{bmatrix} \sigma_r & \tau_{r\theta} & \tau_{rz} \\ \text{symm} & \sigma_\theta & \tau_{\theta z} \\ & & \sigma_z' \end{bmatrix} = \begin{bmatrix} 0 & 0 & \tau_{rz} \\ \text{symm} & \sigma_\theta & \tau_{\theta z} \\ & & \sigma_z' \end{bmatrix} \quad (12)$$

We now rotate the cylindrical coordinate system about the tunnel radius vector r by an angle α (Fig. 7) in order to be able to retrieve the additional three components of the stress tensor in the z -direction ($\sigma_z, \tau_{zx}, \tau_{zy}$). The rotation matrix for this case is

$$Q_{ij} = \begin{bmatrix} 1 & 0 & 0 \\ 0 & \cos \alpha & -\sin \alpha \\ 0 & \sin \alpha & \cos \alpha \end{bmatrix} \quad (13)$$

According to the second-order tensor (matrix) transformation rule of isotropic Cartesian coordinates, we obtain:

$$\begin{aligned} \sigma(r'', \theta'', z'') &= Q_{ij} \times \sigma(r, \theta, z) \times Q_{ij}^T \\ \begin{bmatrix} \sigma_r'' & \tau_{r\theta}'' & \tau_{rz}'' \\ \text{symm} & \sigma_\theta'' & \tau_{\theta z}'' \\ & & \sigma_z'' \end{bmatrix} &= \begin{bmatrix} 1 & 0 & 0 \\ 0 & \cos \alpha & -\sin \alpha \\ 0 & \sin \alpha & \cos \alpha \end{bmatrix} \\ &\times \begin{bmatrix} 0 & 0 & \tau_{rz} \\ \text{symm} & \sigma_\theta & \tau_{\theta z} \\ & & \sigma_z' \end{bmatrix} \times \begin{bmatrix} 1 & 0 & 0 \\ 0 & \cos \alpha & -\sin \alpha \\ 0 & \sin \alpha & \cos \alpha \end{bmatrix}^T \\ &= \begin{bmatrix} 0 & 0 & 0 \\ -\sin \alpha \tau_{zr} & \cos \alpha \sigma_\theta - \sin \alpha \tau_{\theta z} & \cos \alpha \tau_{\theta z} - \sin \alpha \sigma_z' \\ \cos \alpha \tau_{rz} & \sin \alpha \sigma_\theta + \cos \alpha \tau_{\theta z} & \sin \alpha \tau_{\theta z} + \cos \alpha \sigma_z' \end{bmatrix} \\ &\times \begin{bmatrix} 1 & 0 & 0 \\ 0 & \cos \alpha & \sin \alpha \\ 0 & -\sin \alpha & \cos \alpha \end{bmatrix} \end{aligned} \quad (14)$$

Table 1
Concentrated results of six theoretical flat jack tests performed around a circular opening.

Test no.	P1	P2	P3	P4	P5	P6
Rotation angle $\theta/^\circ$	55	55	90	120	335	335
Rotation angle $\alpha/^\circ$	45	0	75	0	135	0
Measured cancellation pressure in slot/MPa	-4.5	-6.0	-4.5	-4.0	-5.0	-3.5

includes all six components of the stress tensor:

$$\begin{aligned} \sigma_\theta'' &= [(1 - 2 \cos 2\theta)\cos^2 \alpha - 2\nu \cos 2\theta \sin^2 \alpha] \sigma_x \\ &+ [(1 + \cos 2\theta)\cos^2 \alpha + 2\nu \cos 2\theta \sin^2 \alpha] \sigma_y + \sin^2 \alpha \sigma_z - 4 \sin \\ &\times 2\theta (\cos^2 \alpha + \nu \sin^2 \alpha) \tau_{xy} + \sin \theta \sin 2\alpha \tau_{zx} - \cos \theta \sin 2\alpha \tau_{zy} \end{aligned} \quad (16)$$

To conclude this section, we show that by performing six flat jack tests that provide σ_θ'' at different positions and orientations around the tunnel we can recover the six components of the *in-situ* stress tensor ($\sigma_x, \sigma_y, \sigma_z, \tau_{xy}, \tau_{zx}, \tau_{zy}$) by means of the standard Flat Jack method. Although from a theoretical standpoint only six tests are required, it would be prudent to perform more than six tests in field applications, in case one or two tests were not performed strictly according to the suggested methods, or have failed.

4. Worked example

Consider the flat jack testing array shown in Fig. 9. Assuming the material is isotropic we need to solve a six-variable linear equation as shown in Eq. (17) below utilizing a software package such as MATLAB, for example.

$$\begin{bmatrix} \sigma_{\theta 1} \\ \sigma_{\theta 2} \\ \sigma_{\theta 3} \\ \sigma_{\theta 4} \\ \sigma_{\theta 5} \\ \sigma_{\theta 6} \end{bmatrix} = \begin{bmatrix} (1 - 2 \cos 2\theta_1)\cos^2 \alpha_1 - 2\nu & (1 + \cos 2\theta_1)\cos^2 \alpha_1 + 2\nu & \sin^2 \alpha_1 - 4 \sin & \sin \theta_1 \sin 2\alpha_1 - \cos \theta_1 \sin 2\alpha_1 \\ \cos 2\theta_1 \sin^2 \alpha_1 & \cos 2\theta_1 \sin^2 \alpha_1 & 2\theta_1 (\cos^2 \alpha_1 + \nu \sin^2 \alpha_1) & \\ (1 - 2 \cos 2\theta_2)\cos^2 \alpha_2 - 2\nu & (1 + \cos 2\theta_2)\cos^2 \alpha_2 + 2\nu & \sin^2 \alpha_2 - 4 \sin & \sin \theta_2 \sin 2\alpha_2 - \cos \theta_2 \sin 2\alpha_2 \\ \cos 2\theta_2 \sin^2 \alpha_2 & \cos 2\theta_2 \sin^2 \alpha_2 & 2\theta_2 (\cos^2 \alpha_2 + \nu \sin^2 \alpha_2) & \\ (1 - 2 \cos 2\theta_3)\cos^2 \alpha_3 - 2\nu & (1 + \cos 2\theta_3)\cos^2 \alpha_3 + 2\nu & \sin^2 \alpha_3 - 4 \sin & \sin \theta_3 \sin 2\alpha_3 - \cos \theta_3 \sin 2\alpha_3 \\ \cos 2\theta_3 \sin^2 \alpha_3 & \cos 2\theta_3 \sin^2 \alpha_3 & 2\theta_3 (\cos^2 \alpha_3 + \nu \sin^2 \alpha_3) & \\ (1 - 2 \cos 2\theta_4)\cos^2 \alpha_4 - 2\nu & (1 + \cos 2\theta_4)\cos^2 \alpha_4 + 2\nu & \sin^2 \alpha_4 - 4 \sin & \sin \theta_4 \sin 2\alpha_4 - \cos \theta_4 \sin 2\alpha_4 \\ \cos 2\theta_4 \sin^2 \alpha_4 & \cos 2\theta_4 \sin^2 \alpha_4 & 2\theta_4 (\cos^2 \alpha_4 + \nu \sin^2 \alpha_4) & \\ (1 - 2 \cos 2\theta_5)\cos^2 \alpha_5 - 2\nu & (1 + \cos 2\theta_5)\cos^2 \alpha_5 + 2\nu & \sin^2 \alpha_5 - 4 \sin & \sin \theta_5 \sin 2\alpha_5 - \cos \theta_5 \sin 2\alpha_5 \\ \cos 2\theta_5 \sin^2 \alpha_5 & \cos 2\theta_5 \sin^2 \alpha_5 & 2\theta_5 (\cos^2 \alpha_5 + \nu \sin^2 \alpha_5) & \\ (1 - 2 \cos 2\theta_6)\cos^2 \alpha_6 - 2\nu & (1 + \cos 2\theta_6)\cos^2 \alpha_6 + 2\nu & \sin^2 \alpha_6 - 4 \sin & \sin \theta_6 \sin 2\alpha_6 - \cos \theta_6 \sin 2\alpha_6 \\ \cos 2\theta_6 \sin^2 \alpha_6 & \cos 2\theta_6 \sin^2 \alpha_6 & 2\theta_6 (\cos^2 \alpha_6 + \nu \sin^2 \alpha_6) & \end{bmatrix} \begin{bmatrix} \sigma_x \\ \sigma_y \\ \sigma_z \\ \tau_{xy} \\ \tau_{zx} \\ \tau_{zy} \end{bmatrix} \quad (17)$$

Solving Eq. (14), the desired σ_θ'' can therefore be expressed as

$$\begin{aligned} \sigma_\theta'' &= [-\sin \alpha \tau_{zr} \cos \alpha \sigma_\theta - \sin \alpha \tau_{\theta z} \cos \alpha \tau_{\theta z} - \sin \alpha \sigma_z'] \cdot \begin{bmatrix} 0 \\ \cos \alpha \\ -\sin \alpha \end{bmatrix} \\ \sigma_\theta'' &= \cos^2 \alpha \sigma_\theta - \sin 2\alpha \tau_{\theta z} + \sin^2 \alpha \sigma_z' \end{aligned} \quad (15)$$

Substituting Eq. (6) and the expressions for σ_θ and σ_z' shown in Eq. (11) into Eq. (15), we obtain the desired solution for σ_θ'' which

In Table 1, the results of six theoretical flat jack tests are presented for four different θ angles and four different α angles. We will assume here that Poisson's ratio is $\nu=0.3$. Note that the positions and rotation angles (θ, α) are displayed in Fig. 9.

Using the data obtained in the six measurement points around the tunnel the complete far field stress tensor may be recovered by solving a system of linear equations as shown in Eq. (17). For the test results shown in Table 1 the obtained *in-situ* stress tensor is

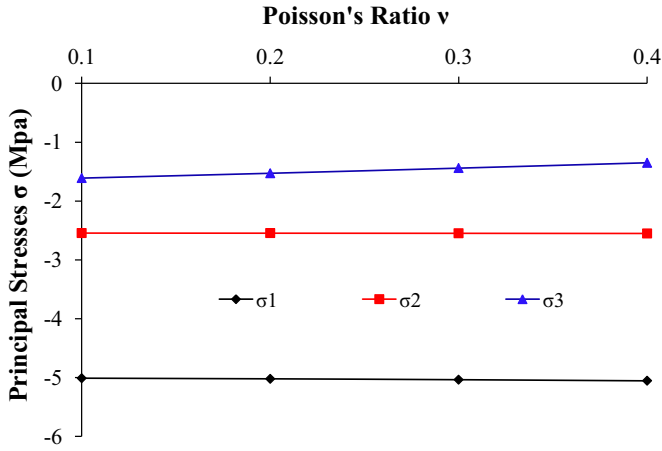


Fig. 10. Sensitivity of analytical solution to the value of Poisson's ratio.

$$\sigma = \begin{bmatrix} -2.4993 & 0.2889 & 0.0208 \\ & -2.2318 & -1.4312 \\ \text{symm} & & -4.2953 \end{bmatrix} \quad (18)$$

The magnitude and orientation of the principal stresses are readily determined by finding the eigenvalues and eigenvectors of Eq. (18):

$$\sigma_{1,2,3} = \begin{bmatrix} -5.0369(\sigma_1) & 0 & 0 \\ 0 & -2.5487(\sigma_2) & 0 \\ 0 & 0 & -1.4409(\sigma_3) \end{bmatrix}$$

$$n_{1,2,3} = \begin{bmatrix} n_1 & n_2 & n_3 \\ -0.0595 & 0.9716 & 0.2292 \\ 0.4585 & -0.1773 & 0.8708 \\ 0.8867 & 0.1569 & -0.4350 \end{bmatrix} \quad (19)$$

A sensitivity analysis of the analytical solution with respect to the value of Poisson's ratio reveals that it is not very sensitive to the value of ν (Fig. 10).

5. Summary and conclusions

A complete analytical solution has been derived for obtaining the six components of the far field *in-situ* stress tensor based on six flat jack tests performed around a circular tunnel. In the analysis, we assume a Continuous, Homogenous, Isotropic, Linear Elastic (CHILE) rock mass. No assumptions need to be made with respect to the orientation of the initial far field stresses and the slots do not have to be perpendicular to the tunnel axis. We have shown that a minimum of three different θ positions around the tunnel axis and a minimum of three α inclinations around the tunnel radius vector are required for obtaining the complete stress tensor. The proposed analytical solution is not very sensitive to the

assumed value of Poisson's ratio for the rock mass near the tunnel.

Acknowledgments

We thank the Israel Commission for Higher Education for a post-doctoral fellowship awarded for excellent doctoral students from China (No. 850203241) through Ben-Gurion University of the Negev. Two anonymous reviewers are thanked for critical reading of an early version of this technical note and for their insightful comments.

Appendix. A. Analytical solution for the stress components in cross section of a circular tunnel using superposition of far field stresses

To obtain the stress distribution around a hole in an infinite elastic plate consisting of isotropic material we will investigate the contribution of each of the stresses separately using the principle of superposition (Fig. A1).

A.1. Horizontal tension

Fig A1(b) represents a plate with a hole submitted to a horizontal uniform tension σ_x in the x -direction. The original and primed coordinate systems shown in Fig. A2 establish the angles between the various axes. The rotation matrix is given by [e.g. Ref. [14]]:

$$Q_{ij} = \begin{bmatrix} \cos \theta & \sin \theta \\ -\sin \theta & \cos \theta \end{bmatrix} \quad (A.1)$$

Transformation of field variables between rectangular and cylindrical coordinates [14] gives in our case:

$$\begin{bmatrix} \sigma_r & \tau_{r\theta} \\ \tau_{r\theta} & \sigma_\theta \end{bmatrix} = Q_{ij} \times \sigma_{(x,y)} \times Q_{ij}^T$$

$$= \begin{bmatrix} \cos \theta & \sin \theta \\ -\sin \theta & \cos \theta \end{bmatrix} \begin{bmatrix} \sigma_x & 0 \\ 0 & 0 \end{bmatrix} \begin{bmatrix} \cos \theta & \sin \theta \\ -\sin \theta & \cos \theta \end{bmatrix}^T$$

$$= \begin{bmatrix} \cos \theta \sigma_x & 0 \\ -\sin \theta \sigma_x & 0 \end{bmatrix} \begin{bmatrix} \cos \theta & -\sin \theta \\ \sin \theta & \cos \theta \end{bmatrix} \quad (A.2)$$

Solving Eq. (A.2) for the case of horizontal uniform tension, we obtain:

$$\sigma_r = \cos^2 \theta \sigma_x = \frac{1}{2}(1 + \cos 2\theta)\sigma_x = \frac{1}{2}\sigma_x + \frac{1}{2} \cos 2\theta \sigma_x$$

$$\tau_{r\theta} = -\sin \theta \cos \theta \sigma_x = -\frac{1}{2} \sin 2\theta \sigma_x \quad (A.3)$$

The result obtained in Eq. (A.3) can be arrived at by superposition of two cases, the first due to the normal constant component $(1/2)\sigma_x$ (Fig. A3b) and the other due to the normal stress

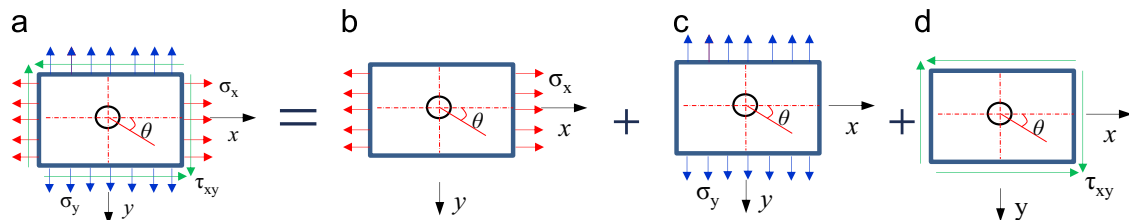


Fig. A1. Superposition of stresses. (a) Natural stress, (b) horizontal stress, (c) vertical stress, and (d) Pure shear.

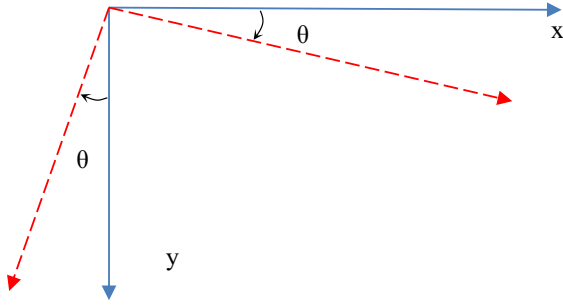


Fig. A2. Coordination transformation.

$(1/2)\cos 2\theta\sigma_x$ and the shear stress $(-1/2)\sin 2\theta\sigma_x$ components (Fig. A3c).

The equation of compatibility [15] is as follows:

$$\nabla^4\phi = \left(\frac{d^2}{dr^2} + \frac{1}{r} \frac{d}{dr} + \frac{1}{r^2} \frac{d^2}{d\theta^2} \right)^2 \phi = 0 \tag{A.4}$$

where ϕ is a general stress function. In the case of horizontal uniform tension (Fig. A3(b)) where the stress function depends on r only, the general solution of Eq. (A.4) can be resolved by means of Euler differential equation and MATLAB to obtain the following general stress function:

$$\phi = A \log r + Br^2 \log r + Cr^2 + D \tag{A.5}$$

Using the stress function, we can obtain the stress and the displacement components:

$$\left. \begin{aligned} \sigma_r &= \frac{1}{r} \frac{\partial \phi}{\partial r} + \frac{1}{r^2} \frac{\partial^2 \phi}{\partial \theta^2} = \frac{A}{r^2} + B(1 + 2 \log r) + 2C \\ \sigma_\theta &= \frac{\partial^2 \phi}{\partial r^2} = -\frac{A}{r^2} + B(3 + 2 \log r) + 2C \\ \tau_{r\theta} &= 0 \end{aligned} \right\} \tag{A.6}$$

$$u_\theta = \frac{4Br\theta}{E} + Hr - I \sin \theta + K \cos \theta \tag{A.7}$$

Note that in the displacement u_θ , the term $4Br\theta/E$ is not single-valued after making a complete circle around the ring. Therefore, we let $B=0$ and σ_r in Eq. (A.6) reduces to $\sigma_r = A/r^2 + 2C$. From the boundary conditions in Fig. A3(b) ($\sigma_r(r=a) = 0$; $\sigma_r(r=b) = (1/2)\sigma_x$) we obtain the constants $A = -(a^2/2)\sigma_x$ and $C = (1/4)\sigma_x$ for this case. For the far field stresses we get:

$$\sigma_r = \frac{\sigma_x}{2} \left(1 - \frac{a^2}{r^2} \right) \quad \sigma_\theta = \frac{\sigma_x}{2} \left(1 + \frac{a^2}{r^2} \right) \quad \tau_{r\theta} = 0 \tag{A.8}$$

Considering now the contribution of the normal force $(1/2)\cos 2\theta\sigma_x$ and the shearing force $(-1/2)\sin 2\theta\sigma_x$ in Fig. A3(c), we may assume a stress function such as:

$$\phi = f(r)\cos 2\theta \tag{A.9}$$

Substituting Eq. (A.9) into the general form of the compatibility

Eq. (A.4), we can express the general solution of Eq. (A.9) as follows:

$$\phi = \left(Ar^2 + Br^4 + C\frac{1}{r^2} + D \right) \cos 2\theta \tag{A.10}$$

Combined with a stress function [15], the corresponding stress components are:

$$\left. \begin{aligned} \sigma_r &= \frac{1}{r} \frac{\partial \phi}{\partial r} + \frac{1}{r^2} \frac{\partial^2 \phi}{\partial \theta^2} = - \left(2A + \frac{6C}{r^4} + \frac{4D}{r^2} \right) \cos 2\theta \\ \sigma_\theta &= \frac{\partial^2 \phi}{\partial r^2} = \left(2A + 12Br^2 + \frac{6C}{r^4} \right) \cos 2\theta \\ \tau_{r\theta} &= \frac{\partial}{\partial r} \left(\frac{1}{r} \frac{\partial \phi}{\partial \theta} \right) = \left(2A + 6Br^2 - \frac{6C}{r^4} - \frac{2D}{r^2} \right) \sin 2\theta \end{aligned} \right\} \tag{A.11}$$

The constants of integration can be determined by using the boundary conditions as shown in Fig. A3(c), $\sigma_r(r=a) = 0$; $\sigma_r(r=b) = (1/2)\cos 2\theta\sigma_x$; $\tau_{r\theta}(r=a) = 0$; $\tau_{r\theta}(r=b) = -(1/2)\sin 2\theta\sigma_x$:

$$A = -\frac{1}{4}\sigma_x \quad B = 0 \quad C = -\frac{a^2}{4}\sigma_x \quad D = \frac{a^2}{2}\sigma_x \tag{A.12}$$

Substituting these constants into Eq. (A.11), and adding the stresses produced by the uniform tension $(1/2)\sigma_x$ on the outer boundary calculated from Eq. (A.8), we obtain the stress components of Fig. A3(b) due to horizontal tension:

$$\left. \begin{aligned} \sigma_r^{\text{Horizontalstress}} &= \frac{\sigma_x}{2} \left(1 - \frac{a^2}{r^2} \right) + \frac{\sigma_x}{2} \left(1 - \frac{a^2}{r^2} \right) \left(1 - \frac{3a^2}{r^2} \right) \cos 2\theta \\ \sigma_\theta^{\text{Horizontalstress}} &= \frac{\sigma_x}{2} \left(1 + \frac{a^2}{r^2} \right) - \frac{\sigma_x}{2} \left(1 + \frac{3a^2}{r^2} \right) \cos 2\theta \\ \tau_{r\theta}^{\text{Horizontalstress}} &= \tau_{\theta r}^a = -\frac{\sigma_x}{2} \left(1 - \frac{a^2}{r^2} \right) \left(1 + \frac{3a^2}{r^2} \right) \sin 2\theta \end{aligned} \right\} \tag{A.13}$$

A.2. Vertical tension

Consider now a plate with a hole submitted to a vertical uniform tension σ_y (Fig. A1c). Transformation of field variables between rectangular and cylindrical coordinates (Fig. A2), gives in this case [14]:

$$\begin{aligned} \begin{bmatrix} \sigma_r & \tau_{r\theta} \\ \tau_{r\theta} & \sigma_\theta \end{bmatrix} &= Q_{ij} \times \sigma_{(x,y)} \times Q_{ij}^T \\ &= \begin{bmatrix} \cos \theta & \sin \theta \\ -\sin \theta & \cos \theta \end{bmatrix} \begin{bmatrix} 0 & 0 \\ 0 & \sigma_y \end{bmatrix} \begin{bmatrix} \cos \theta & \sin \theta \\ -\sin \theta & \cos \theta \end{bmatrix}^T \\ &= \begin{bmatrix} 0 & \sin \theta \sigma_y \\ 0 & \cos \theta \sigma_y \end{bmatrix} \begin{bmatrix} \cos \theta & -\sin \theta \\ \sin \theta & \cos \theta \end{bmatrix} \end{aligned} \tag{A.14}$$

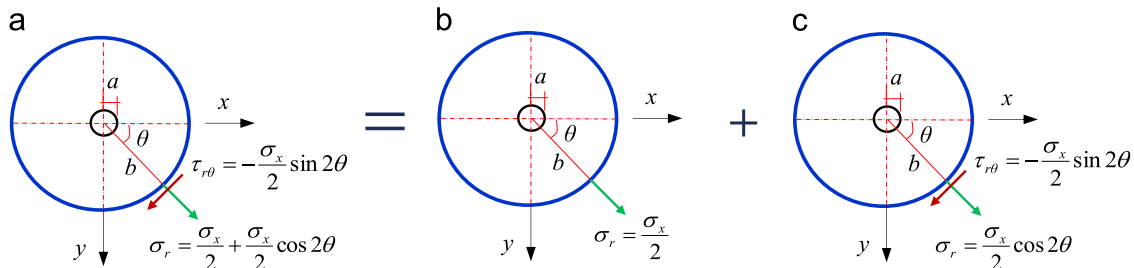


Fig. A3. Stress state of circular hole under horizontal stress in plate. (a) Stress at radius b. (b) Normal forces. (c) Normal force and shearing force.

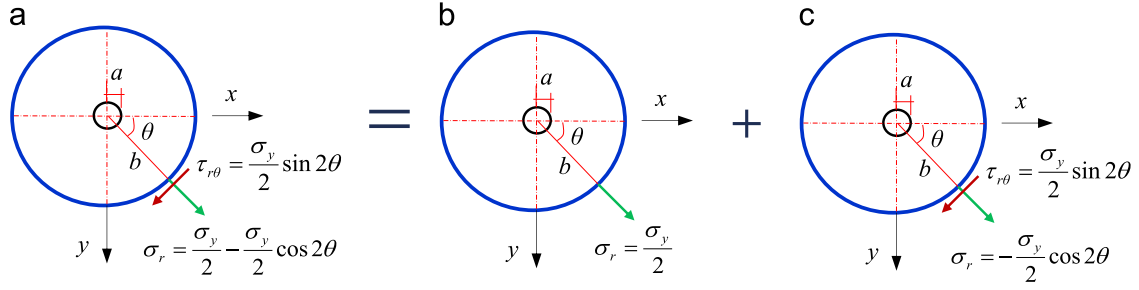


Fig. A4. Stress state of circular hole under vertical stress in plate. (a) Stress at radius b . (b) Normal forces. (c) Normal force and shearing force.

Solving Eq. (A.14) in terms of cylindrical coordinates, we get:

$$\begin{aligned} \sigma_r &= \sigma_y \sin^2 \theta = \frac{1}{2} \sigma_y (1 - \cos 2\theta) = \frac{1}{2} \sigma_y - \frac{1}{2} \sigma_y \cos 2\theta \\ \tau_{r\theta} &= \sigma_y \sin \theta \cos \theta = \frac{1}{2} \sigma_y \sin 2\theta \end{aligned} \quad (\text{A.15})$$

The result obtained in Eq. (A.15) can be arrived at by superposition of two contributions as shown in Fig. A4(b) and (c) namely, the first due to the normal component $(1/2)\sigma_y$ and the remaining part due to the normal stress $-(1/2)\sigma_y \cos 2\theta$ and the shear stress $(1/2)\sigma_y \sin 2\theta$ components.

The constant component $(1/2)\sigma_y$ of the normal forces in Fig. A4(b) is similar to Eq. (A.8) in Fig. A3(b). Therefore, we obtain:

$$\sigma_r = \frac{\sigma_y}{2} \left(1 - \frac{a^2}{r^2}\right) \quad \sigma_\theta = \frac{\sigma_y}{2} \left(1 + \frac{a^2}{r^2}\right) \quad \tau_{r\theta} = 0 \quad (\text{A.16})$$

Considering now the contribution of the normal force $-(1/2)\sigma_y \cos 2\theta$ and the shearing force $(1/2)\sigma_y \sin 2\theta$ in Fig. A4(c), we assume stresses that may be derived from a stress function which is of the same form as of Eq. (A.9). Therefore, the corresponding stress components around the hole are identical to Eq. (A.11).

The constants of integration for this case can be determined by solving the boundary conditions as shown in Fig. A4(c), $\sigma_{r(r=a)} = 0$; $\sigma_{r(r=b)} = -(1/2)\cos 2\theta \sigma_y$; $\tau_{r\theta(r=a)} = 0$; $\tau_{r\theta(r=b)} = (1/2)\sin 2\theta \sigma_y$:

$$A = \frac{1}{4} \sigma_y \quad B = 0 \quad C = \frac{a^4}{4} \sigma_y \quad D = -\frac{a^2}{2} \sigma_y \quad (\text{A.17})$$

Substituting the constants of integration into Eq. (A.11) and adding the stresses produced by the uniform tension $(1/2)\sigma_y$ on the outer boundary calculated from Eq. (A.16), we obtain the stress components due to vertical tension in Fig. A1(c):

$$\left. \begin{aligned} \sigma_r^{\text{Verticalstress}} &= \frac{\sigma_y}{2} \left(1 - \frac{a^2}{r^2}\right) - \frac{\sigma_y}{2} \left(1 - \frac{a^2}{r^2}\right) \left(1 - \frac{3a^2}{r^2}\right) \cos 2\theta \\ \sigma_\theta^{\text{Verticalstress}} &= \frac{\sigma_y}{2} \left(1 + \frac{a^2}{r^2}\right) + \frac{\sigma_y}{2} \left(1 + \frac{3a^2}{r^2}\right) \cos 2\theta \\ \tau_{r\theta}^{\text{Verticalstress}} &= \frac{\sigma_y}{2} \left(1 - \frac{a^2}{r^2}\right) \left(1 + \frac{3a^2}{r^2}\right) \sin 2\theta \end{aligned} \right\} \quad (\text{A.18})$$

A.3. Pure shear

Fig. A1(d) represents a plate with a hole submitted to pure shear τ_{xy} . Transformation of field variables between rectangular and cylindrical coordinates (Fig. A2) gives [14]:

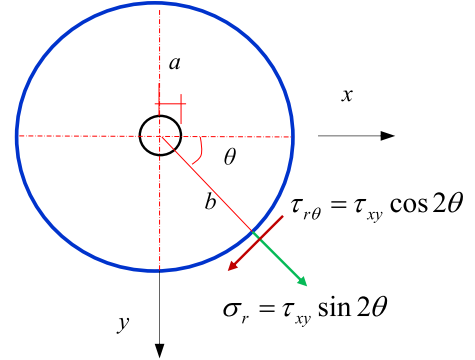


Fig. A5. Corresponding stress as uniform far-field tension and shearing loading.

$$\begin{aligned} \begin{bmatrix} \sigma_r & \tau_{r\theta} \\ \tau_{\theta r} & \sigma_\theta \end{bmatrix} &= \begin{bmatrix} \cos \theta & \sin \theta \\ -\sin \theta & \cos \theta \end{bmatrix} \\ &\times \begin{bmatrix} 0 & \tau_{xy} \\ \tau_{yx} & 0 \end{bmatrix} \begin{bmatrix} \cos \theta & \sin \theta \\ -\sin \theta & \cos \theta \end{bmatrix}^T \\ &= \begin{bmatrix} \sin \theta \tau_{yx} & \cos \theta \tau_{xy} \\ \cos \theta \tau_{yx} & -\sin \theta \tau_{xy} \end{bmatrix} \begin{bmatrix} \cos \theta & -\sin \theta \\ \sin \theta & \cos \theta \end{bmatrix} \\ \sigma_r &= \tau_{xy} \sin 2\theta \\ \tau_{r\theta} &= \tau_{xy} \cos 2\theta \end{aligned} \quad (\text{A.19})$$

Fig. A5 shows a large plate in a state of pure shear τ_{xy} , perturbed by a hole of radius a . Due to the normal stress $\sigma_r = \tau_{xy} \sin 2\theta$ and shearing stress $\tau_{r\theta} = \tau_{xy} \cos 2\theta$ in Fig. A5, we assume stresses that may be derived from a stress function of the form:

$$\phi = f(r) \sin 2\theta \quad (\text{A.20})$$

Substituting the stress function from Eq. (A.20) into the compatibility Eq. (A.4), we can express the general solution of Eq. (A.20) as:

$$\phi = \left(Ar^2 + Br^4 + C \frac{1}{r^2} + D \right) \sin 2\theta \quad (\text{A.21})$$

Combined with a stress function [15], the corresponding stress components are:

$$\left. \begin{aligned} \sigma_r &= \frac{1}{r} \frac{\partial \phi}{\partial r} + \frac{1}{r^2} \frac{\partial^2 \phi}{\partial \theta^2} = - \left(2A + \frac{6C}{r^4} + \frac{4D}{r^2} \right) \sin 2\theta \\ \sigma_\theta &= \frac{\partial^2 \phi}{\partial r^2} = \left(2A + 12Br^2 + \frac{6C}{r^4} \right) \sin 2\theta \\ \tau_{r\theta} &= - \frac{\partial}{\partial r} \left(\frac{1}{r} \frac{\partial \phi}{\partial \theta} \right) = \left(2A + 6Br^2 - \frac{6C}{r^4} - \frac{2D}{r^2} \right) \cos 2\theta \end{aligned} \right\} \quad (\text{A.22})$$

The constants of integration can be determined by the

boundary conditions shown in Fig. A5, $\sigma_r(r=a) = 0$;
 $\sigma_r(r=b) = \tau_{xy} \sin 2\theta$; $\tau_{r\theta}(r=a) = 0$; $\tau_{r\theta}(r=b) = \tau_{xy} \cos 2\theta$:

$$A = -\frac{1}{2}\tau_{xy} \quad B = 0 \quad C = -\frac{a^4}{2}\tau_{xy} \quad D = a^2\tau_{xy} \quad (\text{A.23})$$

Substituting the constants of integration into Eq. (A.22), we obtain the stress components due to pure shear stress:

$$\begin{aligned} \sigma_r^{\text{Pureshear}} &= \tau_{xy} \left(1 - \frac{a^2}{r^2}\right) \left(1 - \frac{3a^2}{r^2}\right) \sin 2\theta \\ \sigma_\theta^{\text{Pureshear}} &= -\tau_{xy} \left(1 + \frac{3a^4}{r^4}\right) \sin 2\theta \\ \tau_{r\theta}^{\text{Pureshear}} &= \tau_{xy} \left(1 - \frac{a^2}{r^2}\right) \left(1 + \frac{3a^2}{r^2}\right) \cos 2\theta \end{aligned} \quad (\text{A.24})$$

The result obtained here for pure shear is identical to the expression obtained in Ref. [16] using the Fourier method.

Finally, subsequent to the analysis of horizontal, vertical and shear stress respectively, the state of stress around the hole can be obtained by superposition as follows:

$$\begin{aligned} \sigma &= \sigma^{\text{Horizontalstress}} + \sigma^{\text{Verticalstress}} + \sigma^{\text{Purestress}} \\ &= \text{Eqs. (A.13)} + \text{Eqs. (A.18)} + \text{Eqs. (A.24)} \end{aligned} \quad (\text{A.25})$$

$$\left. \begin{aligned} \sigma_r &= \frac{\sigma_x + \sigma_y}{2} \left(1 - \frac{a^2}{r^2}\right) + \frac{\sigma_x - \sigma_y}{2} \left(1 - \frac{a^2}{r^2}\right) \left(1 - \frac{3a^2}{r^2}\right) \cos 2\theta \\ &\quad + \tau_{xy} \left(1 - \frac{a^2}{r^2}\right) \left(1 - \frac{3a^2}{r^2}\right) \sin 2\theta \\ \sigma_\theta &= \frac{\sigma_x + \sigma_y}{2} \left(1 + \frac{a^2}{r^2}\right) - \frac{\sigma_x - \sigma_y}{2} \left(1 + \frac{3a^2}{r^2}\right) \cos 2\theta \\ &\quad - \tau_{xy} \left(1 + \frac{3a^4}{r^4}\right) \sin 2\theta \\ \tau_{r\theta} &= \tau_{r\theta} \\ &= -\frac{\sigma_x - \sigma_y}{2} \left(1 - \frac{a^2}{r^2}\right) \left(1 + \frac{3a^2}{r^2}\right) \sin 2\theta + \tau_{xy} \left(1 - \frac{a^2}{r^2}\right) \\ &\quad \left(1 + \frac{3a^2}{r^2}\right) \cos 2\theta \end{aligned} \right\} \quad (\text{A.26})$$

References

1. Kim K, Franklin JA. Suggested methods for rock stress determination. *Int J Rock Mech Min Sci*. 1987;24:53–73.
2. Fairhurst C. Stress estimation in rock: a brief history and review. *Int J Rock Mech Min* 2003;40:957–73.
3. Mayer A, Habib P, Marchand R. Underground rock pressure testing. In: *Proceedings of the International Conference on Rock Pressure and Support in Workings*; Liège1951.
4. Rocha M.A. New technique for applying the method of the flat jack in the determination of stress inside rock masses. In: *Proceedings of the First International Congress Rock Mechanics*. Lisbon; 1966, pp 57–65.
5. Hoskins ER. An investigation of the flat jack method of measuring rock stress. *Int J Rock Mech Min Sci* 1966;3:249–64.
6. Amadei B, Stephansson O. *Rock Stress and Its Measurement*. London: Chapman & Hall; 1997.
7. Goodman RE. *Introduction to Rock Mechanics*. 2nd ed., New York: Wiley; 1989.
8. Pinto JL, Cunha AP. Rock stresses determinations with the STT and SFJ techniques. In: *Proceedings of the Rock Stress and Rock Stress Measurements*. Lulea; 1986, pp 253–260.
9. Franco JAD, Armelin JL, Santiago JAF, Telles JCF, Mansur WJ. Determination of the natural stress state in a Brazilian rock mass by back analysing excavation measurements: a case study. *Int J Rock Mech Min* 2002;39:1005–32.
10. Figueiredo B, Cornet FH, Lamas L, Muralha J. Determination of the stress field in a mountainous granite rock mass. *Int J Rock Mech Min Sci* 2014;72:37–48.
11. Homand F, Souley M, Gaviglio P, Mamane I. Modelling natural stresses in the arc syncline and comparison with in situ measurements. *Int J Rock Mech Min* 1997;34:1091–107.
12. Faiella D, Manfredini G, Rossi PP. In situ flat jack tests: analysis of results and critical assessment. In: *Proceedings of the International Symposium on Soil and Rock Investigations by In situ Testing*. Paris; 1983, pp 507–512.
13. Kirsch G. Die theorie der elastizität und die bedürfnisse der festigkeitslehre. *Veit Ver Deut Ing* 1898;42:797–807.
14. Sadd MH. *Elasticity Theory, Applications, and Numerics*. Amsterdam: Elsevier Academic Press; 2005.
15. Timoshenko SP, Goodier JN. *Theory of Elasticity*. 3rd ed., New York: McGraw-Hill; 1970.
16. Barber JR. *Elasticity*. Kluwer Academic Publishers; 1992.